# Joint least-squares inversion of up- and down-going signal for ocean bottom data sets

*Mandy Wong, Biondo Biondi, and Shuki Ronen*

## ABSTRACT

We present a joint least-squares inversion method for imaging the acoustic primary (up-going) and mirror (down-going) signals for ocean-bottom seismic processing. Joint inversion combines the benefits of wider illumination from the mirror signal and better signal-to-noise ratio from the primary signal into one image. Results from two modified 2D Marmousi models show a better illumination of the subsurface and improved resolution in geologically complex areas.

## INTRODUCTION

Ocean-bottom seismic (OBS) acquisition is an established technology in which seismometers are placed at the sea bottom and shots are fired at the sea surface. In areas congested by platforms or other obstacles, ocean bottom seismic is advantageous because it is operated by small boats without cumbersome towed streamers. Such a geometry enables OBS acquisition to provide wide-azimuth illumination, shear-wave recording, a quieter recording environment, higher-resolution data and improved repeatability. Therefore, it is used for imaging in obstructed oilfields and for time-lapse monitoring of hydrocarbon reservoirs.

There are different processing schemes for ocean bottom data. The traditional way, inherited from surface seismic processing, is to remove all free-surface multiples and to migrate only with the primary signal (Wang et al., 2009). Therefore, initial work on OBS data processing has been dedicated to the removal of free-surface multiples. One way to attenuate strong free-surface multiples is to combine the geophone and hydrophone recordings to eliminate the receiver ghost and the water column reverberations, a technique known as PZ summation (Barr and Sander, 1989; Soubaras, 1996; Schalkwijk et al., 1999). Such a technique uses the polarity difference between a scalar measurement (pressure) and a vector measurement (velocity). As an alternative to PZ summation, Sonneland and Berg (1987) and Amundsen (2001) address free-surface multiples with the theory of up-down deconvolution in both layered and complex media. In this approach, not only are all free-surface multiples attenuated, but also de-ghosting and signature deconvolution are conducted in a single step.

While multiples are often treated as noise, they are formed by the same source signal as primaries but travel along different paths in the medium. The receiver ghost, also

known as the mirror signal, is the next order of reflection beyond the primaries with an additional reflection off the sea surface. In a deep water OBS survey, the source grid has a much wider lateral extend than the receiver grid. Therefore, the subsurface reflection point of the receiver ghost is located at greater distances from the receiver station than the primaries Figure 1. Therefore, the mirror signal can provide a wider subsurface illumination than the primaries if the energy is properly migrated. Several authors have used the mirror signal in the migration of OBS data (Godfrey et al., 1998; Ronen et al., 2005; Grion et al., 2007; Dash et al., 2009).

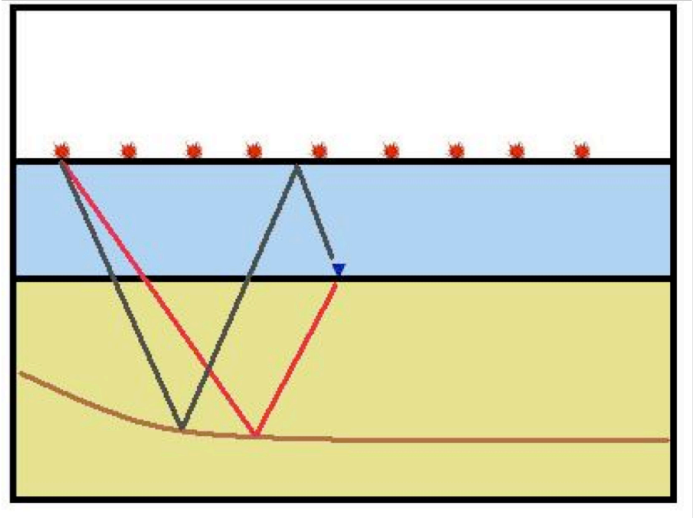

Figure 1: The subsurface reflection point of the receiver ghost, also known as the mirror signal (in black), is located at a greater distance from the receiver station than the primary signal (in red). For a deep water OBS survey, the source grid has a much wider lateral extend than the receiver grid. This translates to a wider subsurface illumination for the mirror signal than the primaries. [**NR**]

While most authors conclude that the mirror image gives a better result than the conventional primary image, the information in the primary image is also valuable. The primary ray path is shorter than the mirror ray path, which contributes to a higher signal-to-noise ratio in the primary signal. In a common receiver gather, the illumination points of the subsurface by each source-receiver pair are closer together in the primary reflection than in the mirror reflection. This translates to higher image quality in the region illuminated by the primary. Instead of treating the primary image and the mirror image separately, we propose an iterative linear least-squares inversion scheme that combines the primary and the mirror image. Such an inversion can improve the structure and aperture of the seismic images by using two sets of signals: the up-going primaries and the down-going mirror signals.

Muijs et al. (2007) made an early attempt to image primary and free-surface multiples together. It requires the data to be decomposed into up-going and down-going constituents, followed by downward extrapolation and a 2D deconvolution based imaging condition. While this technique is computationally efficient, its image contains

crosstalk artifacts caused by interference of up-going and down-going waves not associated with the same subsurface reflector. In contrast to Muijs' method, joint inversion can optimally combine structural information provided by two types of reflection that are free from crosstalk.

In this paper, we focus on the joint inversion of the acoustic (P) wave signal. We first discuss the theory of the joint linear least-squares inversion. We then apply the inversion scheme to two modified versions of the 2D Marmousi model and show the overall improvement of the joint inversion result.

## JOINT INVERSION OF UP/DOWN-GOING P WAVE

Joint inversion of up- and down-going signals for ocean-bottom data can potentially be a better imaging technique than migrating either signal alone, because it combines information from both sets of signals. Figure 4 summarizes the processing scheme for our algorithm. Ocean bottom data are first separated into acoustic up- and down-going components above the seafloor. The decomposed signals are then inverted to yield one optimally combined reflectivity image. The objective function for such an inversion is:

$$0 \approx \begin{bmatrix} \mathbf{L}_{\uparrow} \\ \mathbf{L}_{\downarrow} \end{bmatrix} \mathbf{m} - \begin{bmatrix} \mathbf{d}_{\uparrow} \\ \mathbf{d}_{\downarrow} \end{bmatrix}, \tag{1}$$

where $\mathbf{L}_{\uparrow}$ and $\mathbf{L}_{\downarrow}$ are modeling operators that produce up-going data ($\mathbf{d}_{\uparrow}$) and down-going data ($\mathbf{d}_{\downarrow}$) from the model space ($\mathbf{m}$). The up- and down-going operators can be defined in many ways with varying levels of difficulty and practicality. We use the adjoint of the acoustic reverse time migration (RTM) operator to formulate $\mathbf{L}_{\uparrow}$ and $\mathbf{L}_{\downarrow}$. Two modified computational grids are used to forward model the lowest order of up- and down-going signals, namely the primary and the receiver ghost. The formulation of the modeling and its adjoint (RTM) operator is summarized in Figure 2 and Figure 3.

In the modified computational grid as shown in Figure 2, the primary signal is obtained by the cross-correlation of the source wavefields with the reflectivity. For the down-going receiver ghost, the receiver nodes are placed at twice the water depth, which effectively represents a reflection off the sea surface.

## NUMERICAL EXAMPLE

We demonstrate the joint inversion of up- and down-going signals using two test cases, both modified from the 2D Marmousi model. The first example has a dense source and receiver spacing. It shows the improvement of joint inversion under optimal conditions. The second example explores the results of our algorithm when the source and receiver spacing are large.

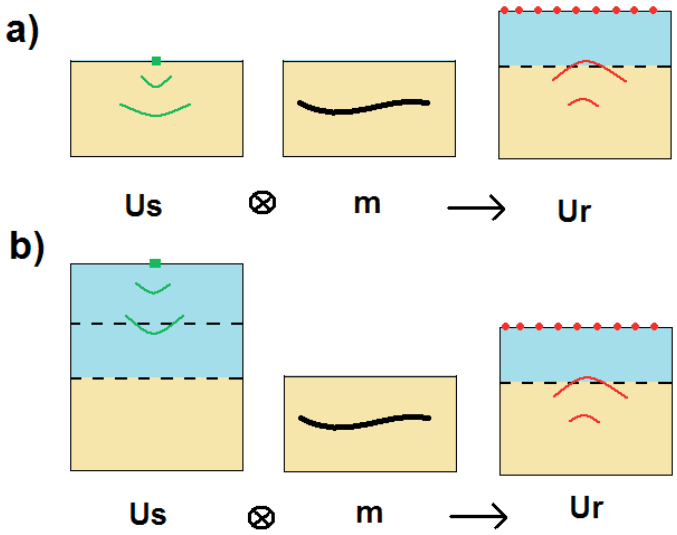


Figure 2: Forward modeling of (a) primary-only and (b) mirror-only data. The algorithm involves cross-correlating the source wavefield ($U_s$) with the reflectivity model ($m$) to generate the receiver wavefield ($U_r$). Reciprocity is used here where the data, in common-receiver domain, are injected at the source location while the source wavelet is injected at the receiver location. Cross-correlation is done only with grid points below the seabed. [**NR**]

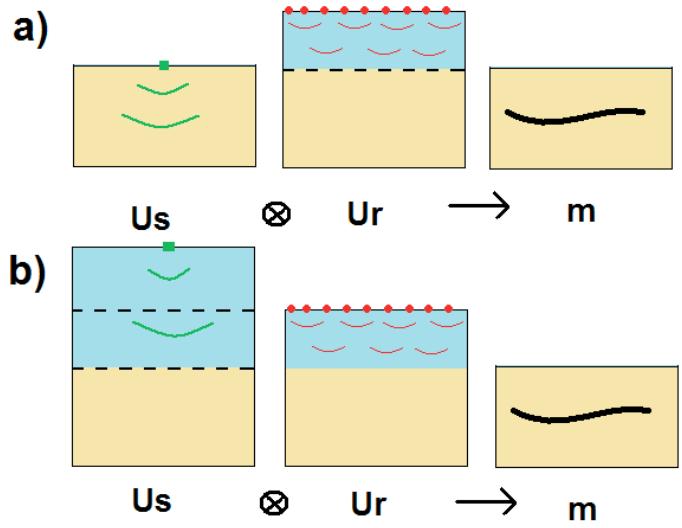


Figure 3: RTM of (a) primary-only and (b) mirror-only data. The algorithm involves cross-correlating the source wave field ($U_s$) with the receiver wave field ($U_r$) to generate the reflectivity model ($m$). Cross-correlation is done only with grid points below the seabed. [**NR**]

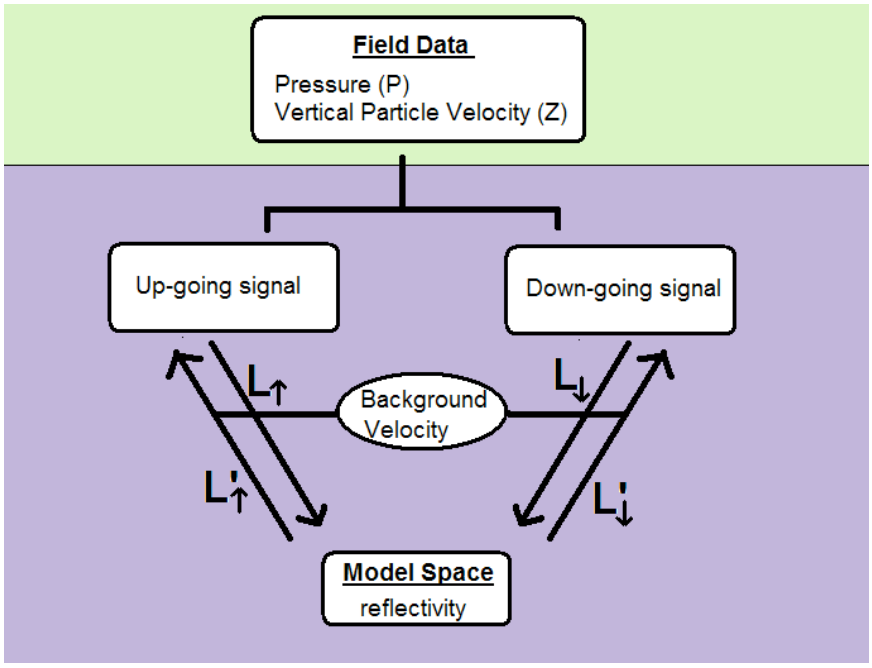


Figure 4: Pressure (P) and vertical particle velocity (Z) data are converted into up- and down-going data. The up- and down-going data are then migrated separately using a modified grid shown in Figure 3. Inversion is performed with residuals in the up/down data domain. [**NR**]

## Marmousi model with dense sampling

Figure 6 (d) shows the reflectivity model used for this example. The model is 2 km deep and 7 km wide with a spacing of 10 m. The ocean floor is not included in this model and is assumed to be flat. However, it is possible to adapt the method to handle an ocean floor with topography. We use a water layer of 500m. All the images are generated in a target-oriented way. That means when we apply the RTM operator, we only cross-correlate regions below the sea-bottom. For simplicity, a constant velocity of 2500 m/s is used for this model.

For the synthetic data, we use the $\mathbf{L}_\uparrow$ and $\mathbf{L}_\downarrow$ defined in the last section to forward model the lowest-order up-going (primary) and down-going (receiver ghost) data. In equation form, this is written as:

$$\begin{aligned} \mathbf{d}_\uparrow^{mod} &= \mathbf{L}_\uparrow \mathbf{m} \\ \mathbf{d}_\downarrow^{mod} &= \mathbf{L}_\downarrow \mathbf{m}. \end{aligned} \tag{2}$$

Shots run from 0 to 7000 m at the sea surface at an interval of 10 m. There are 700 shots in total. For the receiver geometry, we use a receiver spacing of 100 m with ocean bottom nodes located at every grid point from 2500 m to 4400 m. There are

20 nodes in total. Because reciprocity is used later, this geometry is equivalent to having 20 shots at the sea-bottom and 700 receivers at the sea-surface. Figure 5 shows the corresponding up-going and down-going common receiver gathers for a shot at x=3200 m.

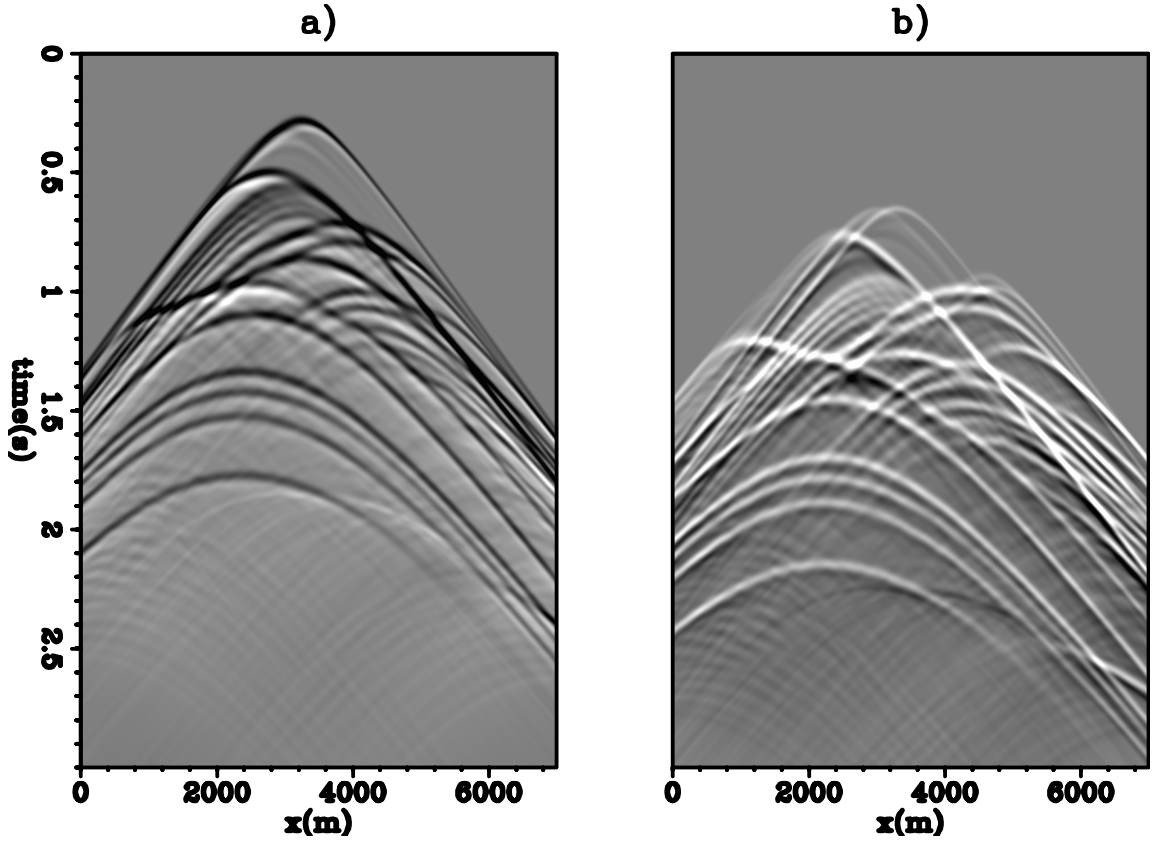


Figure 5: A common-receiver gather taken at x=3200 m: (a) synthetic up-going (primary) data obtained by applying $\mathbf{L}_{\uparrow}$ to the model and (b) synthetic down-going (receiver ghost) data obtained by applying $\mathbf{L}_{\downarrow}$ to the model. [**CR**]

To compare among conventional primary migration, mirror imaging, and joint inversion, we will first present the results of RTM on the conventional primary signal and on the mirror signal. The corresponding image will then be compared to the joint inversion result using both signals.

*Reverse time migration on conventional primary and mirror signals*

In this section, we define the term *up-image* ($\mathbf{m}_{\uparrow}$) to be applying the adjoint of $\mathbf{L}_{\uparrow}$ to the up-going data. The term *down-image* ($\mathbf{m}_{\downarrow}$) is defined similarly. In equation form, this is written as:

$$\begin{aligned} \mathbf{m}_{\uparrow} &= \mathbf{L}'_{\uparrow}\mathbf{d}^{mod}_{\uparrow}, \\ \mathbf{m}_{\downarrow} &= \mathbf{L}'_{\downarrow}\mathbf{d}^{mod}_{\downarrow}. \end{aligned} \tag{3}$$

Panels (a) and (b) of Figure 6 show the corresponding up-image and down-image. Comparing the two images, we can see that wider illumination is achieved by the mirror image. The benefit of the wider aperture is directly correlated with the depth of the sea-bottom. The deeper the sea-bottom, the wider the illumination. On the other hand, a close-up section of the images (Figure 7 (a) and (b)) shows that the up-image has a higher signal-to-noise ratio than the down-image. This is only a synthetic study and we expect the difference will be more apparent with a field dataset.

The goal of joint inversion is to get the best of both worlds. By manipulating two sets of data, we wish to produce a joint image that has both the wide illumination of the down-image and a high signal-to-noise ratio in the region covered by the up-image.

*Joint Inversion Result*

A joint inversion is performed in a least-squares sense with the objective goal described in equation 1. The initial guess is calculated by summing the up-image and the down-image. Panel (c) of Figure 6 shows the image after joint inversion (with 20 iterations). We can see an overall improvement from the migration images in panels (a) and (b) of Figure 6 to the inversion image. We have identified three areas of improvement with the close-up section shown in Figure 7:

1. In panel (c) of Figure 6, the near-surface reflector near z=0-400 m and x=2400-3200 m has a better relative amplitude and is more focused.
2. In panel (c) of Figure 6, the joint image has a wider illumination for the region from x=5000 m to the left and the region from x=2000 m to the right.
3. Figure 7 shows a higher signal-to-noise ratio for the joint image. In addition, the deeper reflector at z=1200-1500 m and x=3200-4000 m are better illuminated in the joint image than in the up-image or the down-image.

This example shows that joint inversion coherently combines information from primary and mirror signal to produce a better illuminated and resolved image. In the next section, we will explore the effect of a sparse geometry between shots and receivers.

## Marmousi model with coarse sampling

In this second example, we increase the spacing of the source and receiver array. There are 22 shots with a spacing of 300m spanning from 500-6800m. We use only

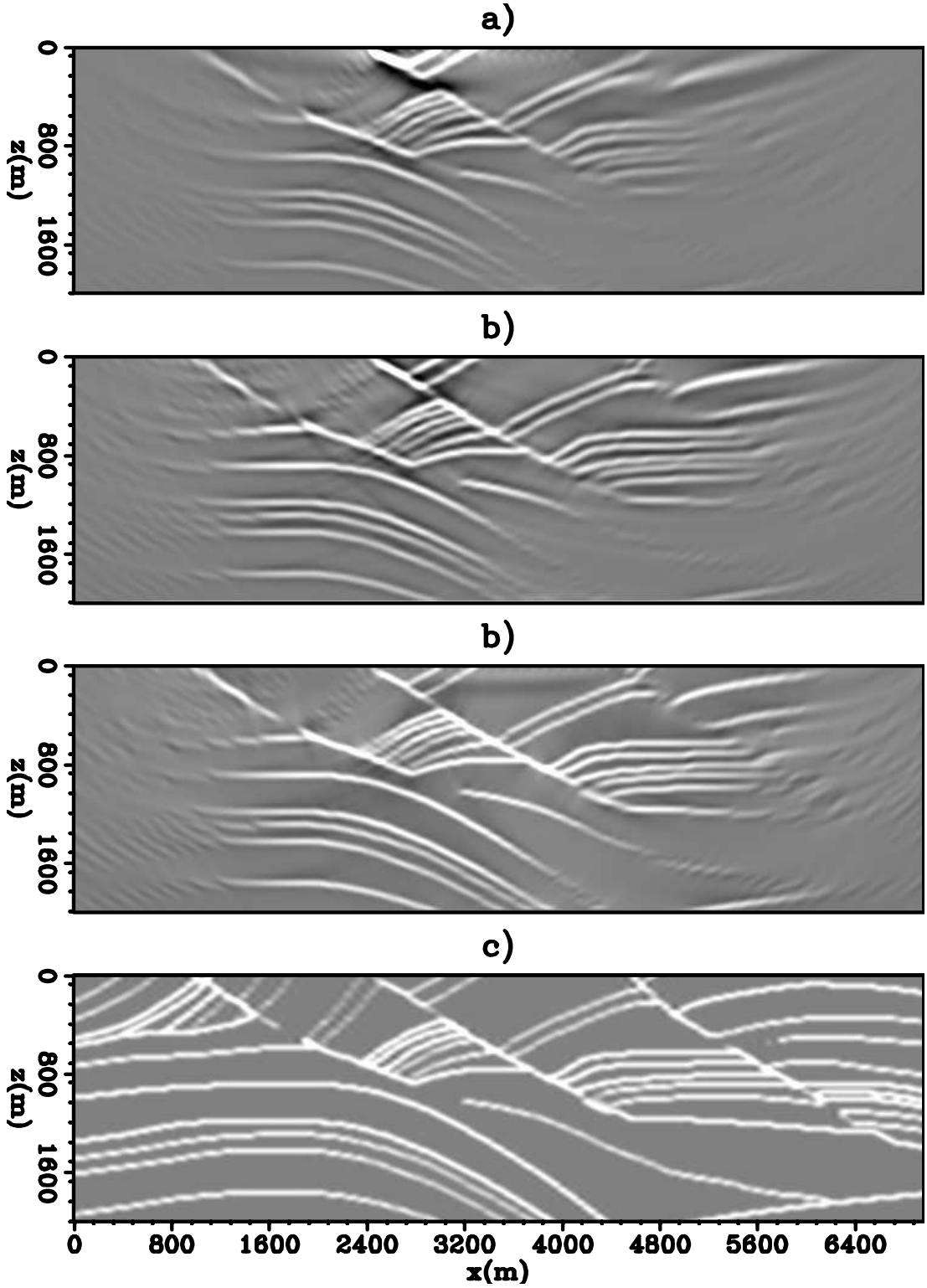


Figure 6: (a) Up-image obtained by calculating $\mathbf{L}_{\uparrow}^{'}\mathbf{d}_{\uparrow}^{mod}$, (b) down-image obtained by calculating $\mathbf{L}_{\downarrow}^{'}\mathbf{d}_{\downarrow}^{mod}$, (c) image obtained by joint inversion, and (d) reflectivity model. [**CR**]

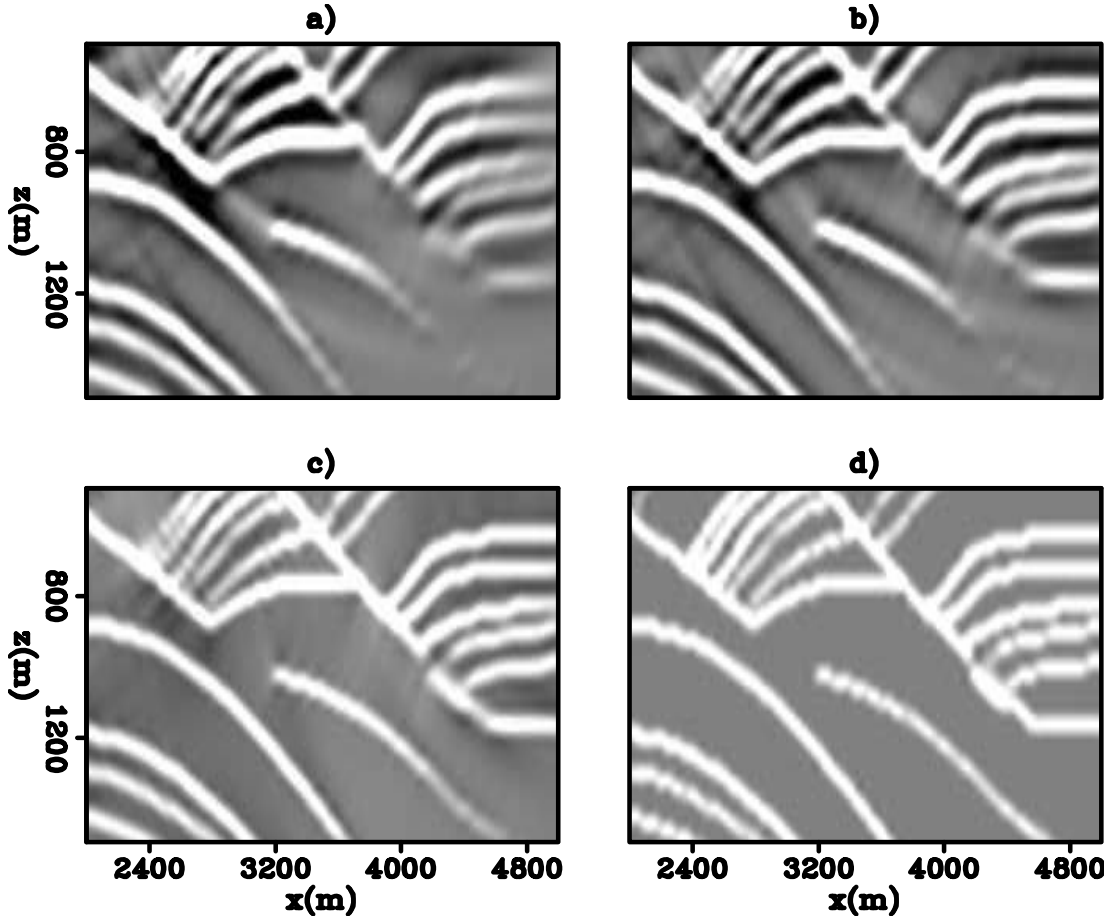


Figure 7: A section of the image cut from x=2500-4500 m and y=500-1500 m. Images are clipped at 90% to contrast the quality among (a) the up-image, (b) the down-image, (c) the joint-image, and (d) the model. [**CR**]

10 receivers that are 400 m apart and span from 2000-5600m. The model grid has a different reflectivity as shown in panel (d) of Figure 8. The rest of the parameters are the same as in the previous example.

Panel (a) and (b) of Figure 8 show the image from migration with the primary signal and with the mirror signal. In the up-image, we can see the strong near-surface amplitude, which is characteristic of the RTM. The down-image is coarse-grained due to the large shot and receiver spacings. Panel (c) of Figure 8 shows the corresponding joint inversion image (with 20 iterations). We can see a dramatic improvement from the joint inversion. This example demonstrates that when the recorded information is limited with respect to the complexity of the subsurface, joint inversion of up- and down-going signal can provide a better illuminated and more refined image.

Figure 9 shows a close up section of Figure 8. It verifies the observation made in the previous example regarding the improvement of the joint-image.

## DISCUSSION AND CONCLUSION

Free-surface multiples in OBS acquisition are often treated as noise. However, because they are formed by the same source signal as primaries but travel along different paths in the medium, they contain information not presence in the primaries. To capitalize on the information provided by both the multiples and the primaries, we have developed a procedure that allows primary and mirror signals to be jointly imaged. While direct migration of the primary has limited illumination aperture, direct migration of the mirror signal is less resolved in complex areas. Joint inversion results in better illumination, improved resolution, and a more balanced amplitude image in geologically complex models.

## REFERENCES

Barr, F. J., and J. I. Sander, 1989, Attenuation of water-column reverberations using pressure and velociy detectors in a water-bottom cable: 59th SEG Annual Meeting Expanded Abstracts, 653–655.

Dash, R., G. Spence, R. Hyndman, S. Grion, Y. Wang, and S. Ronen, 2009, Wide-area imaging from obs multiples: Geophysics, **74**, Q41–Q47.

Godfrey, R., P. Kristiansen, B. Armstrong, M. Cooper, and E. Thorogood, 1998, Imaging the foinaven ghost: 68th SEG Annual Meeting Expanded Abstracts, 1333–1335.

Grion, S., R. Exley, M. Manin, X. Miao, A. Pica, Y. Wang, P. Granger, and S. Ronen, 2007, Mirror imaging of obs data: First Break, **25**, 37–42.

Ronen, S., L. Comeaux, and J. Miao, 2005, Imaging downgoing waves from ocean bottom stations: 75th SEG Annual Meeting Expanded Abstracts, 963–966.

Schalkwijk, K. M., C. P. A. Wapenaar, and D. J. Verschuur, 1999, Application of

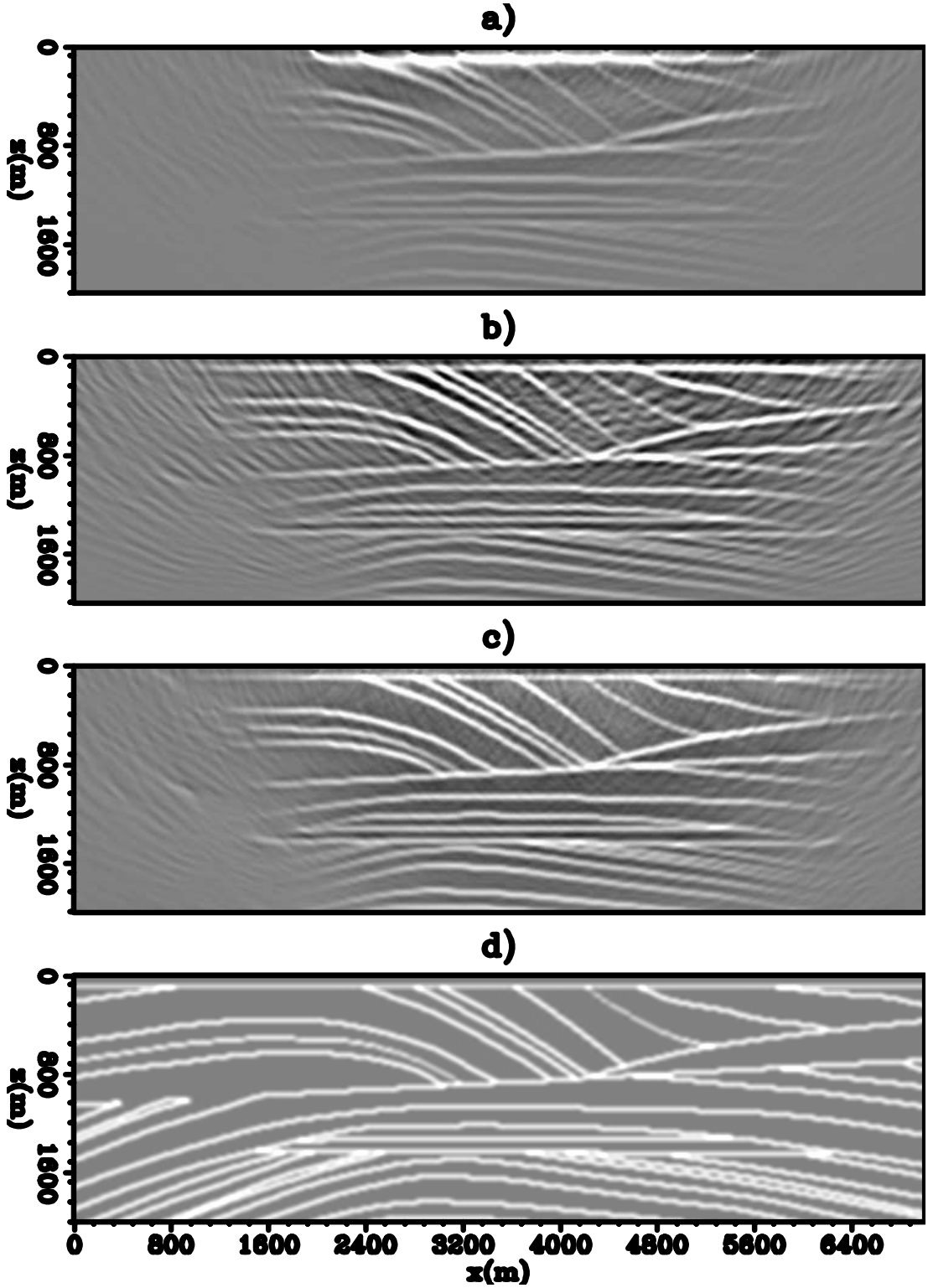


Figure 8: (a) The up-image, (b) the down-image, (c) the joint-image, and (d) the reflectivity model. [**CR**]

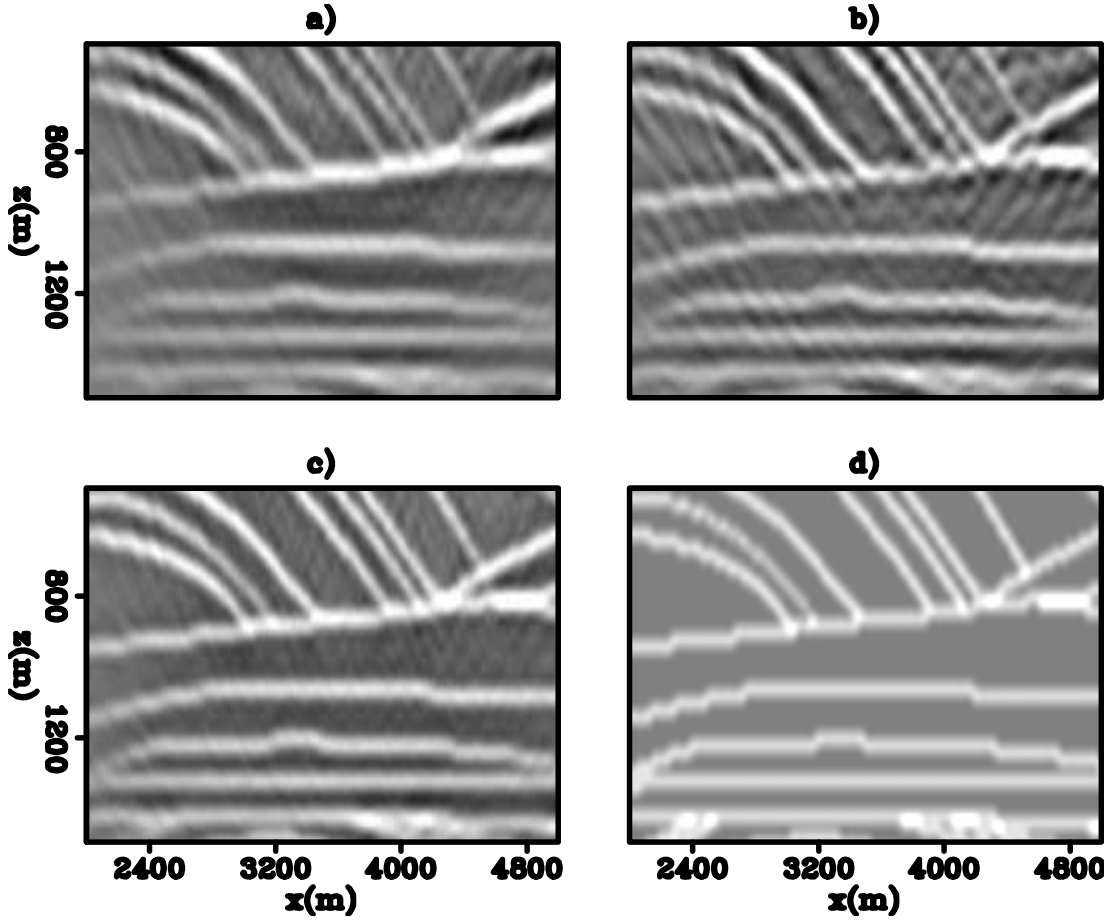


Figure 9: A close-up section of (a)The up-image (b) the down-image (c) the joint-image, and (d) the reflectivity model with coarse sampling. The sections are cut from x=2000-5000 m and y=500-1500 m. [**CR**]

two-step decomposition to multicomponent ocean bottom data: Theory and case study: Journal of Seismic Exploration, **8**, 261–278.

Soubaras, R., 1996, Ocean bottom hydrophone and geophone processing: 66th SEG Annual Meeting Expanded Abstracts, 24–27.

Wang, Y., S. Grion, and R. Bale, 2009, What comes up must have gone down: the principle and application of up-down deconvoluiton for multiple attenuation of ocean bottom data: CSEG Recorder, **34**, 16–20.